

# Tyre Modelling for Use in Vehicle Dynamics Studies

Egbert Bakker and Lars Nyborg

Chassis Engineering

Volvo Car Corp.

**Hans B. Pacejka**

Vehicle Research Laboratory

Delft University of Technology

## ABSTRACT

A new way of representing tyre data obtained from measurements in pure cornering and pure braking conditions has been developed in order to further improve the Dynamic Safety of vehicles. The method makes use of a formula with coefficients which describe some of the typifying quantities of a tyre, such as slip stiffnesses at zero slip and force and torque peak values. The formula is capable of describing the characteristics of side force, brake force and self aligning torque with great accuracy. This mathematical representation is limited to steady-state conditions during either pure cornering or pure braking and forms the basis for a model describing tyre behaviour during combined braking and cornering.

**SAFETY IS A FIELD** which has been given top priority in developing Volvo cars, because people should be able to travel safely and securely. For this reason, the vehicle properties have to be adapted to the driver, so the vehicle will be controllable and its behaviour predictable in all situations. This is called Dynamic Safety and is obtained after optimizing stability, steering and brake performance by tuning chassis and tyre design to each other. Here, the tyre plays a vital role and thorough knowledge of its properties is required. It is therefore necessary to have a proper description of tyre behaviour available. In order to achieve this, a joint project between Volvo and the Delft University of Technology was set up. The

first results of this project have been presented in this paper.

The description and understanding of tyre behaviour should be easily obtainable from measured data. Furthermore, it is desirable that its parameters characterize in some way the typifying quantities of the tyre such as slip stiffnesses at zero slip and peak values of forces and torques. This feature would make it possible to investigate the effect of changes of these quantities upon the handling and stability properties of the vehicle. That is, one might then easily model a hypothetical tyre.

## REPRESENTATION OF TYRE DATA

Three possible ways to represent measured tyre data are in use:

- a) representation by tables,
- b) representation by graphs,
- c) representation by formulae.

The first two possibilities are difficult to handle in theoretical studies and therefore they do not fulfil the requirements mentioned earlier.

Two possibilities may be distinguished for the representation by formulae:

- a) formulae containing series (Fourier, polynomials),
- b) formulae containing special functions.

The use of series has some disadvantages:

- relatively many coefficients are needed to get a close curve fit,
- the resulting curves have a wavy look, which implies that the variation of the slope along the curve differs considerably from that of the

measured data,

- extrapolation beyond the fitted range often yields large deviations,
- in general, the coefficients do not describe the typifying quantities in a recognisable way, which makes it impossible to change these quantities in a controlled, simple way.

A representation with the aid of polynomials is described by Sitchin [1]\*. This investigator attempts to solve some of the problems connected with the use of polynomials by dividing the data into five regions and using a variable format regression equation for each of them. The first two disadvantages could be solved in this way, but the others still remain. A problem appears to show up for the derivative, which is discontinuous at the boundaries of the regions.

The best way to fulfil the requirements is to find a special function, which through its particular structure is capable of describing the measured data with great accuracy and which has parameters related to the typifying quantities in a simple manner.

The formula should, if possible, be able to describe:

- the side force as a function of slip angle,
- the brake force as a function of longitudinal slip,
- the self aligning torque as a function of slip angle.

The side force and self aligning torque are measured during pure cornering (cornering without braking) and the brake force during pure braking (braking without cornering). Both cornering and braking are in steady-state conditions.

A possible special function used by Ruf [2] is a combination of tanh functions. The resulting formula can match side and brake force characteristics rather well. However, the coefficients do not describe the typifying quantities of the tyre in an easy way and therefore these quantities are difficult to recognize and to vary.

#### PROPOSED TYRE FORMULA

The basic form of each of the characteristics of the tyre (cf. Fig.1) suggest the use of the sine function as a first step in developing the final formula as summarized in the Appendix.

\* Numbers in brackets [ ] designate references at the end of the paper.

$$Y = D \sin(BX) \quad (1)$$

with Y standing for either side force, self aligning torque or brake force and X denoting slip angle ( $\alpha$ ) or longitudinal slip ( $\kappa$ ). The longitudinal slip is defined as the ratio of the difference between the speed of rotation of the driven or braked tyre and of the straight free rolling tyre, and the speed of rotation of the straight free rolling tyre, expressed as a percentage. A negative value results from a braking torque. In Eq. (1) D is the peak value and the product DB equals the slip stiffness at zero slip.

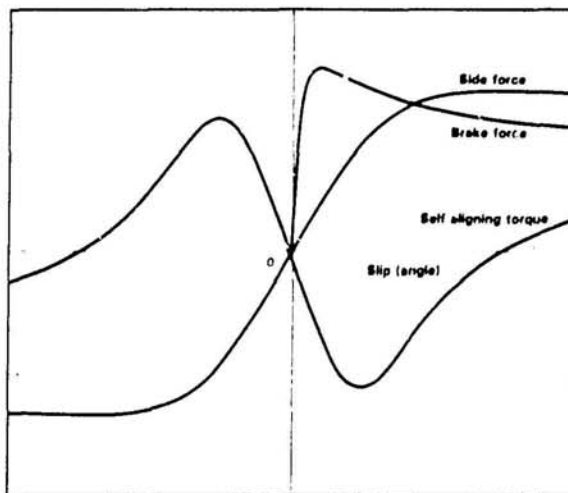


Fig 1. - Steady-state tyre characteristics.

Eq. (1) does not give a good representation for larger values of X. A gradually increasing extension of the X axis appears to be necessary. To accomplish this, the arctan function has been used. The formula (1) now changes into:

$$Y = D \sin(C \arctan(BX)) \quad (2)$$

In Eq. (2) D is still the peak value, the slip stiffness at zero slip is now equal to the product BCD (from now on called the stiffness). The coefficient C governs the shape of the curve. For large values of X, Eq. (2) reduces to:

$$Y = D \sin(\frac{1}{2}\pi C) \quad (3)$$

Consequently, C defines the extent of the sine that will be used and therefore determines the shape of the curve. The value of C makes the curve look like a side force, brake force or a self aligning

torque characteristic (we find for  $C$  in those cases successively: 1.3, 1.65 and 2.4). With  $C$  determined by the shape and  $D$  determined by the peak value, only  $B$  is left to control the stiffness.

Still Eq. (2) is not good enough to describe every possible measured characteristic. There may be a need for an additional coefficient which makes it possible to accomplish a local extra stretch or compression of the curve. The coefficient  $E$  has been introduced into the formula in such a way that stiffness and peak value remain unaffected.

$$Y = D \sin(C \arctan(B\phi))$$

with

$$\phi = (1-E)X + (E/B) \arctan(BX) \quad (4)$$

The influence of  $E$  on the side force characteristic has been shown in Fig. 2. Similar effects occur with the self aligning torque and brake force characteristics.

The result is an equation with four coeff-

icients, which is able to describe all the measured characteristics. The four coefficients are:

- $B$  = stiffness factor
- $C$  = shape factor
- $D$  = peak factor
- $E$  = curvature factor

So far, the characteristics are assumed to pass through the origin. In reality, however, this will not always be the case. Due to ply steer, conicity and rolling resistance, the characteristics will be shifted in the horizontal and/or vertical directions (Fig. 2). In order to fit the measured characteristics, these shifts should be included in the equation. We obtain:

$$Y = D \sin(C \arctan(B\phi)) + S_v \quad (5)$$

with

$$\phi = (1-E)(X + S_h) + (E/B) \arctan(B(X + S_h))$$

$S_h$  = horizontal shift

$S_v$  = vertical shift

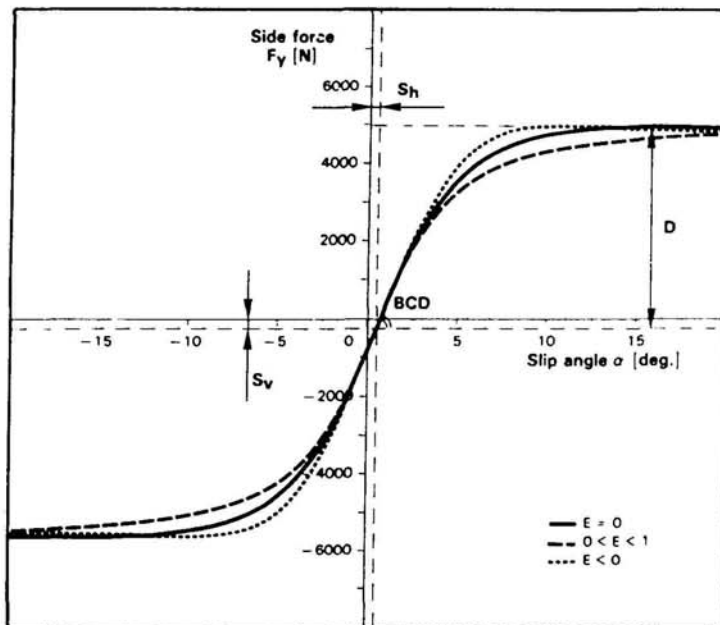


Fig. 2 - Coefficients appearing in tyre formula.

**THE MEASUREMENTS** - Full scale tyre measurements have been carried out on a dry asphalt road. The experiments were conducted with a specially built test trailer under steady-state conditions. The measured quantities are:

- the side force ( $F_y$ ),
- the brake force ( $F_x$ ),
- the self aligning torque ( $M_z$ ).

These forces and torque were measured during pure cornering, pure braking or during combinations of cornering and braking. During cornering, the speed was 70 km/h and during braking 60 km/h. The tests included variations of slip angle (-10 to 14 deg.), vertical load (2, 4, 6, 8 kN) and camber angle (-5, 0, 5 deg.).

The pure cornering tests were carried out by slowly varying the slip angle ( $\alpha$ -sweep) from zero to the maximum value, from there to the minimum value and back to zero again. The measured data was condensed per 1/4 degree intervals to one measured point per interval. After that, corrections were made for load variations, which occurred during the tests, by making use of

quadratical correction curves around the measured points. Finally, the average was taken of two or more  $\alpha$ -sweeps.

The measurements during pure braking were carried out by gradually increasing the brake pressure until wheel lock occurs. The data was collected while the longitudinal slip was increased from 0 to 100% ( $\kappa$ -sweep). Here also a condensation, correction and averaging process has been carried out. The experiments on combined cornering and braking were conducted by doing  $\kappa$ -sweeps at fixed values of the slip angle. The camber angle was fixed at zero degrees.

**FITTING MEASURED DATA** - The data obtained after processing in the way described above has been used as raw input data for the fitting process. An optimization program from the NAG library has been used to obtain the four coefficients and two shifts for every measured characteristic. For one of the measured tyres, the resulting coefficients have been tabulated in Table 1. The vertical shift obtained for the brake forces represents the value for the rolling resistance.

Table 1  
Coefficients for tyre formula (first fit)  
( $\alpha$  [deg.],  $\kappa$  [%])

	LOAD (kN)	B	C	D	E	$S_h$	$S_v$	BCD
$F_y$	2	0.244	1.50	1936	-0.132	-0.280	-118	780.6
	4	0.239	1.19	3650	-0.678	-0.049	-156	1038
	6	0.164	1.27	5237	-1.61	-0.126	-181	1091
	8	0.112	1.36	6677	-2.16	0.125	-240	1017
$M_z$	2	0.247	2.56	-15.53	-3.92	-0.464	-12.5	-9.820
	4	0.234	2.68	-48.56	-0.46	-0.082	-11.7	-30.45
	6	0.164	2.46	-112.5	-2.04	-0.125	-6.00	-45.39
	8	0.127	2.41	-191.3	-3.21	0.009	-4.22	-58.55
$F_x$	2	0.178	1.55	2193	0.432	0.000	25.0	605.0
	4	0.171	1.69	4236	0.619	0.000	70.6	1224
	6	0.210	1.67	6090	0.686	0.000	80.1	2136
	8	0.214	1.78	7711	0.783	0.000	104	2937

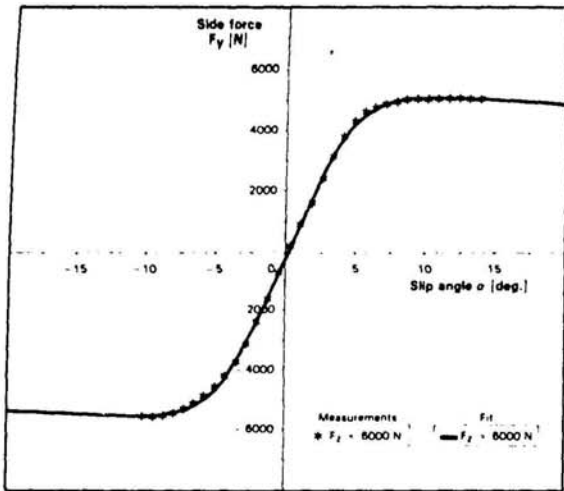


Fig. 3 - Side force characteristic fitted using the tyre formula compared with measured data.

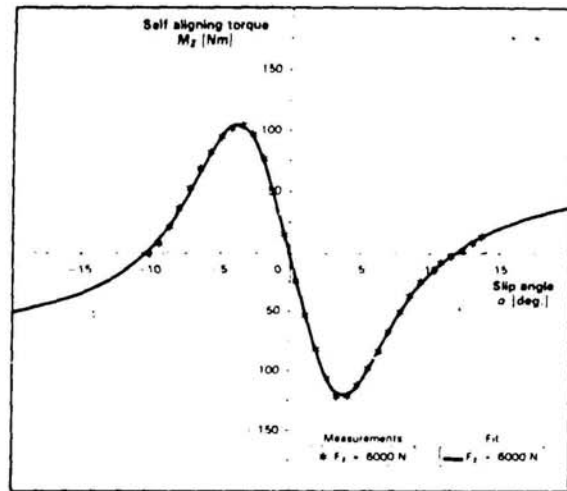


Fig. 4 - Self aligning torque characteristic fitted using the tyre formula compared with measured data.

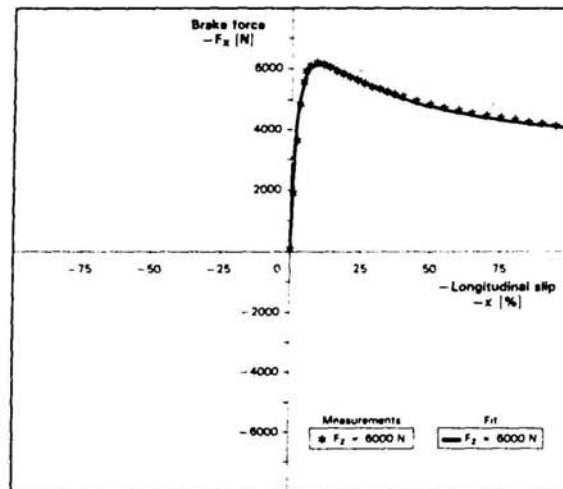


Fig. 5 - Brake force characteristic fitted using the tyre formula compared with measured data.

Figures 3, 4 and 5 show comparisons between measurements (after processing) and fitted characteristics for one specific load. The result is very satisfactory: the formula is able to describe all the measured characteristics.

At the moment, the shifts are not of particular interest for further examination and are therefore put equal to zero (i.e. ply steer, conicity and rolling resistance will not be taken into account). If so required, it is possible to add the shifts later on.

**INFLUENCE OF VERTICAL LOAD** - To reduce the total number of quantified coefficients (Table 1) and to be able to calculate forces and torques at vertical loads which are different from the values used in the measurements, it is necessary to include the vertical load explicitly in the formula. To do so, the coefficients have to be written as a function of the vertical load ( $F_z$ ).

The peak factor (D) as a function of  $F_z$  may be approximately represented by the relationship:

$$D = a_1 F_z^2 + a_2 F_z \quad (6)$$

For the stiffness (BCD) of the side force characteristic (cornering stiffness), we take the formula:

$$BCD = a_3 \sin(a_4 \arctan(a_5 F_z)) \quad (7)$$

and for the stiffness of both brake force (longitudinal slip stiffness) and self aligning torque

(aligning stiffness) characteristics, we use the approximation:

$$BCD = \frac{a_3 F_z^2 + a_4 F_z}{e^{a_5 F_z}} \quad (8)$$

The shape factor (C) appears to be practically independent of  $F_z$ . We take for:

- the side force : C = 1.30
- the brake force : C = 1.65
- the self aligning torque: C = 2.40

The stiffness factor (B) is found by dividing the stiffness by the shape and the peak factor.

$$B = BCD / CD \quad (10)$$

Finally, the curvature factor (E) as a function of  $F_z$  is given by:

$$E = a_6 F_z^2 + a_7 F_z + a_8 \quad (11)$$

After processing the raw data again (corrected for the earlier determined horizontal and vertical shifts) with the aid of the optimization program, the new coefficients are obtained. Table 2 gives the coefficients for the same tyre as in Table 1, but now including the influence of the vertical load.

Table 2  
Coefficients for tyre formula (with load influence)  
( $F_z$  [kN])

	$a_1$	$a_2$	$a_3$	$a_4$	$a_5$	$a_6$	$a_7$	$a_8$
$F_y$	-22.1	1011	1078	1.82	0.208	0.000	-0.354	0.707
$M_z$	-2.72	-2.28	-1.86	-2.73	0.110	-0.070	0.643	-4.04
$F_x$	-21.3	1144	49.6	226	0.069	-0.006	0.056	0.486

Table 3  
Coefficients for tyre formula connected with camber influence  
( $\gamma$  [deg.])

	$a_9$	$a_{10}$	$a_{11}$	$a_{12}$	$a_{13}$
$F_y$	0.028	0.000	14.8	0.022	0.000
$M_z$	0.015	-0.066	0.945	0.030	0.070

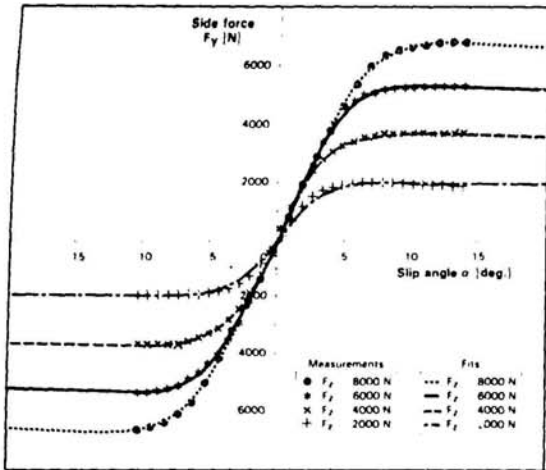


Fig. 6 - Side force characteristics fitted using the tyre formula which includes the influence of the vertical load, compared with measured data.

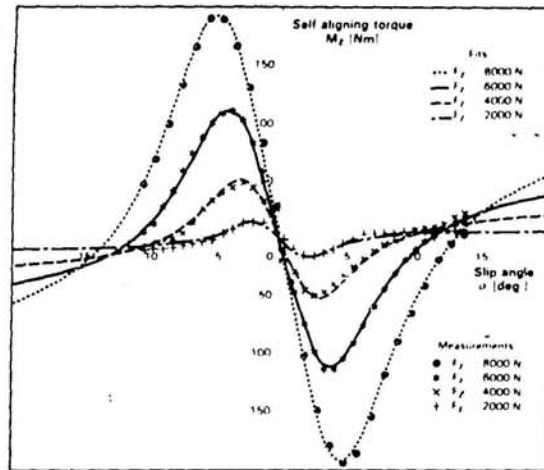


Fig. 7 - Self aligning torque characteristics fitted using the tyre formula which includes the influence of the vertical load, compared with measured data.

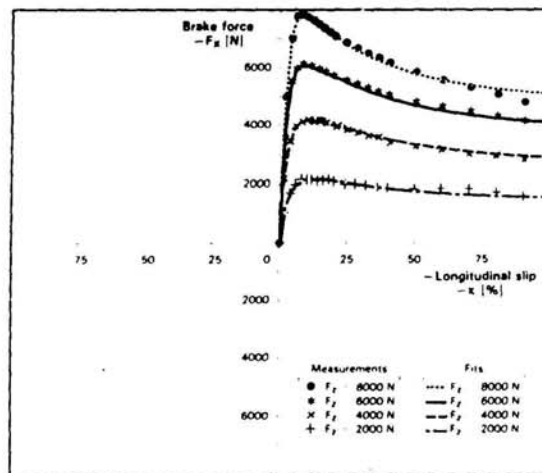


Fig. 8 - Brake force characteristics fitted using the tyre formula which includes the influence of the vertical load, compared with measured data.



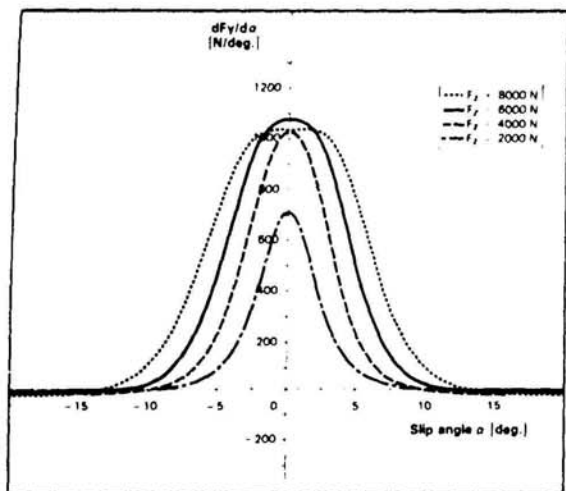


Fig. 9 - Calculated slope of side force characteristics as a function of slip angle for different vertical loads.

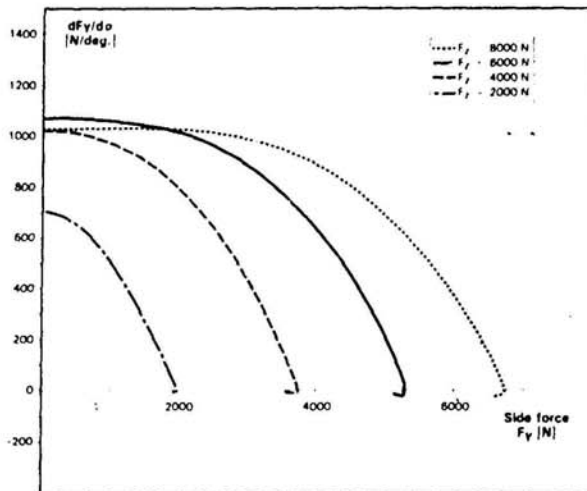


Fig. 10 - Calculated slope of side force characteristics as a function of side force for different vertical loads.

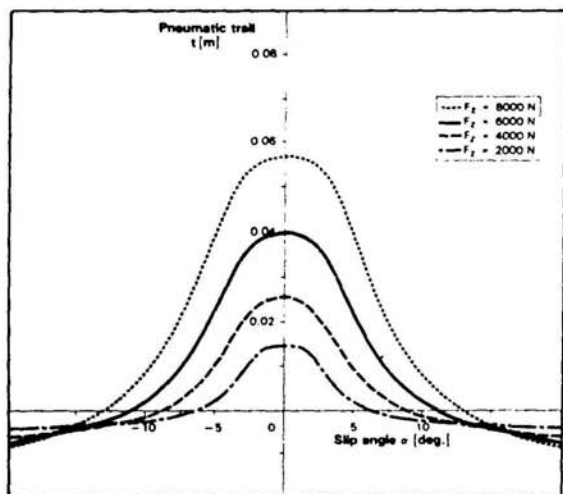


Fig. 11 - Calculated pneumatic trail as a function of slip angle for different loads.

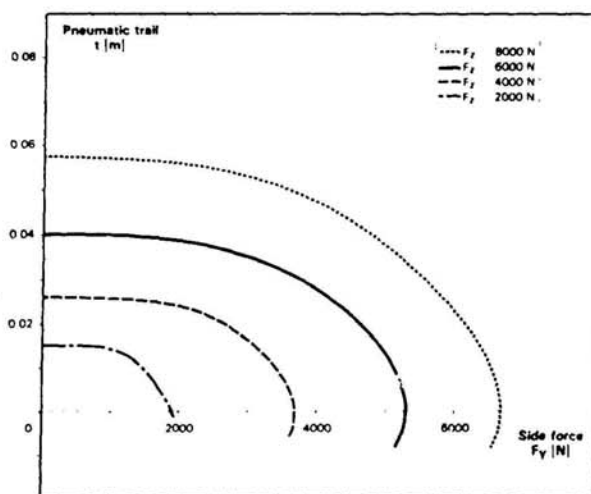


Fig. 12 - Calculated pneumatic trail as a function of side force for different loads.



The new parameter  $a_3$  for the side force indicates the maximum possible cornering stiffness generated by the tyre.

A comparison between measurements and the newly obtained characteristics has been shown in Figs. 6, 7 and 8. The influence of the vertical load is now included without much loss in accuracy.

**INFLUENCE OF CAMBER** - The total number of coefficients to be quantified may be reduced even more by including camber in the formula as well. The influence of camber ( $\gamma$ ) is included by adding two shifts and a possible change in stiffness. The two additional shifts are:

$$\begin{aligned}\Delta S_h &= a_9 \gamma \\ \Delta S_v &= (a_{10} F_z^2 + a_{11} F_z) \gamma\end{aligned}\quad (12)$$

The change in stiffness is obtained by multiplying  $B$  by  $(1 - a_{12} |\gamma|)$ . We have for the increment of  $B$ :

$$\Delta B = -a_{12} |\gamma| B \quad (13)$$

The values of the self aligning torque at higher slip angles will change due to this change in stiffness. To compensate for this effect, the curvature factor  $E$  for  $M_z$  must be divided by  $(1 - a_{13} |\gamma|)$ . For the side force, this compensation is not necessary because the values at higher slip angles are not changed appreciably by changing the stiffness. The values obtained have been shown in Table 3.

At this stage about five thousand measurement points have been reduced to three equations with a total of thirty-one coefficients (coefficients with value zero not included). It is now possible to calculate forces and torques which would arise in circumstances not included in the measurement programme. The equations are summarized in the Appendix.

Beside side force, self aligning torque and brake force, other information may be obtained with the aid of the formula. For instance  $dF_y/da$  as a function of slip angle or as a function of side force (Figs. 9 and 10). It is also possible to calculate the pneumatic trail as a function of slip angle or side force, merely by dividing self aligning torque by the side force (Figs. 11 and 12).

#### MODEL FOR COMBINED CORNERING AND BRAKING

The formulae obtained which describe the

pure cornering and braking conditions, will be used now in a mode which describes the behaviour of the tyre at zero camber angle when a combination of cornering and braking takes place. The modelling process implies the use of the basic tyre modelling theory as described in [3].

Figure 13 shows a top view of a tyre during combined cornering and braking. The force and torque acting on the tyre and the velocity of the wheel have been indicated:

- the total force with components in lateral and longitudinal direction ( $F_y$  and  $F_x$ ),
- the self aligning torque ( $M_z$ ),
- the speed in the direction of travel  $\bar{V}$  which is composed of the slip speed vector ( $\bar{V}_s$ ) and the rolling speed vector ( $\bar{V}_r$ ) of the tyre.

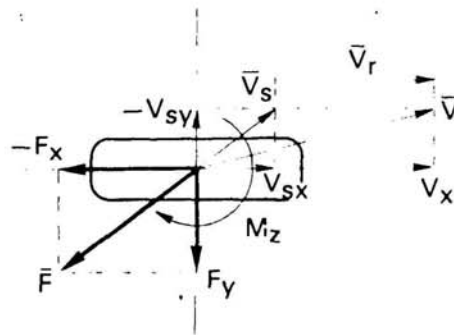


Fig. 13 - Top view of tyre during combined braking and cornering showing velocity and force vector diagrams.

**BRAKE AND SIDE FORCE DURING COMBINED CORNERING AND BRAKING** - If the tyre is assumed to have isotropic properties then the direction of the total force is opposite the slip speed vector. The length of the total force vector is a function of the total newly introduced slip quantity  $\sigma$  [3]. This theoretical slip has components which are defined as follows:

$$\begin{aligned}\sigma_x &= V_{sx}/V_r \\ \sigma_y &= V_{sy}/V_r \\ \sigma &= \sqrt{\sigma_x^2 + \sigma_y^2}\end{aligned}\quad (14)$$

The vector  $\bar{\sigma}$  has the same direction as the slip speed vector  $\bar{V}_s$ . Therefore we find:

$$\begin{aligned}F &= -(\bar{\sigma}/\sigma)F(\sigma) \\ F_x &= -(\sigma_x/\sigma)F(\sigma) \\ F_y &= -(\sigma_y/\sigma)F(\sigma)\end{aligned}\quad (15)$$

The relations between the theoretical slip and the practical slip quantities used earlier ( $\alpha$  and  $\kappa$ ) are:

$$\sigma_x = V_{sx}/V_r = -\kappa/(1 + \kappa) \tag{16}$$

$$\sigma_y = V_{sy}/V_r = -\tan\alpha/(1 + \kappa)$$

where we had:

$$\tan \alpha = -V_{sy}/V_x \tag{17}$$

$$\kappa = -V_{sx}/V_x$$

As stated before, the theory is valid for a tyre with isotropic properties (the same characteristic for side and brake force). But in reality a tyre is not isotropic, so the theory must be adjusted.

Instead of a single characteristic  $F(\sigma)$ , two different characteristics should be used (cf. Lugner [4]):

- for pure cornering:  $F_{y0}(\sigma)$
- for pure braking:  $F_{x0}(\sigma)$

These characteristics are called the original basic curves. The total force may now be derived as follows:

$$\begin{aligned} F_x &= -(\sigma_x/\sigma) F_{x0}(\sigma) \\ F_y &= -(\sigma_y/\sigma) F_{y0}(\sigma) \end{aligned} \tag{18}$$

$$F = \sqrt{F_x^2 + F_y^2}$$

The original basic curves are obtained by calculating  $F_x$  and  $F_y$  in pure conditions and writing them as a function of the theoretical slip with the aid of Eq. (16). Figure 14 shows some of these characteristics for different vertical loads.

A problem of physical nature arises when the values of the slip connected with the peak values of  $F_{x0}$  and  $F_{y0}$  differ considerably from each other. At a slip  $\sigma$  in between these two peaks, we have the situation that total slip would occur on one curve and partial sliding on the other. In reality, the tyre has one total condition of sliding. To solve this problem a new slip quantity is defined which normalizes the theoretical slip. This new slip is called the normalized slip  $\sigma^*$ . The normalized slip is obtained by dividing  $\sigma$  by the slip value which occurs at the peak of the characteristic. We designate these values of slip as  $\sigma_{xm}$  and  $\sigma_{ym}$  for the  $F_x$  and the  $F_y$  characteristics respectively. The components of the normalized slip read:

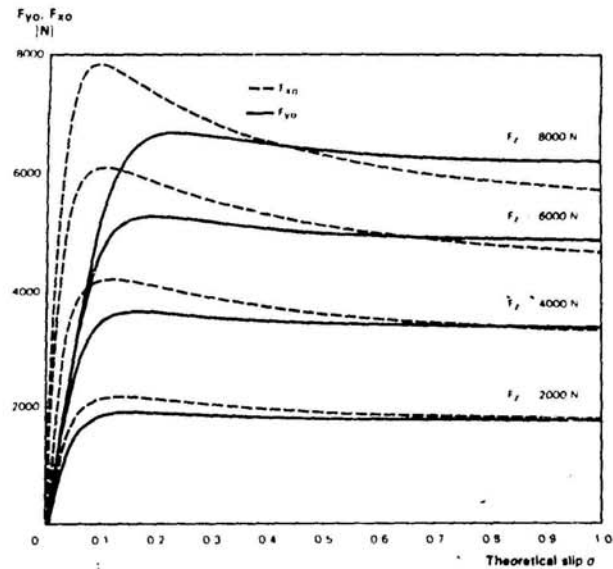


Fig. 14 - Original calculated basic characteristics.

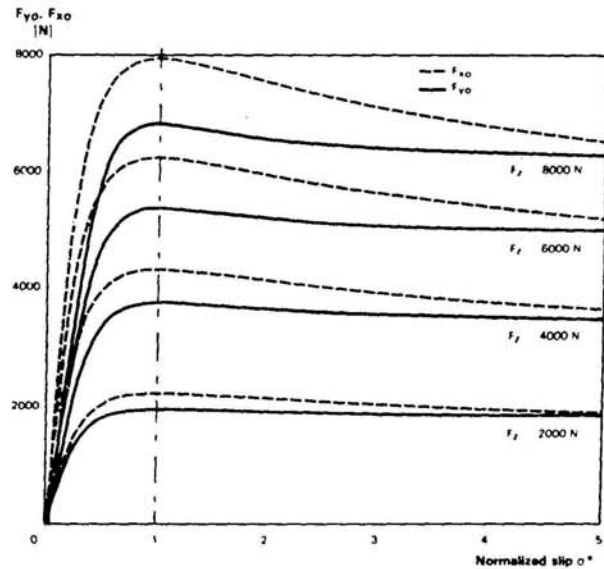


Fig. 15 - Normalized basic characteristics.

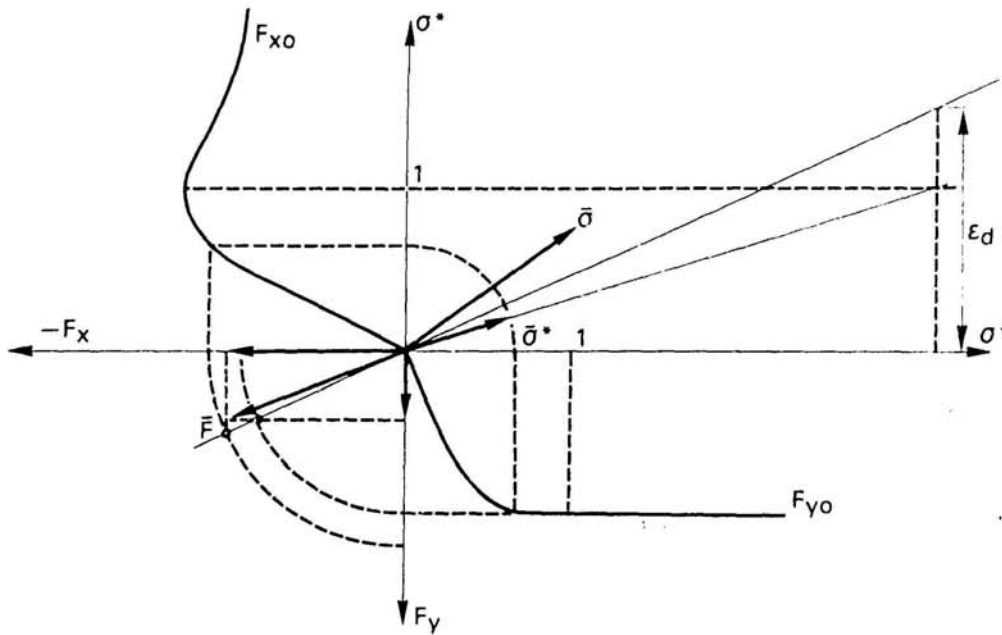


Fig. 16 - Visualization of determination of magnitude and direction of the total horizontal force  $\bar{F}$  using the normalized basic characteristics, starting out from a given normalized slip vector (cf. Figs. 17, 18 for the factor  $\epsilon_d$ ).

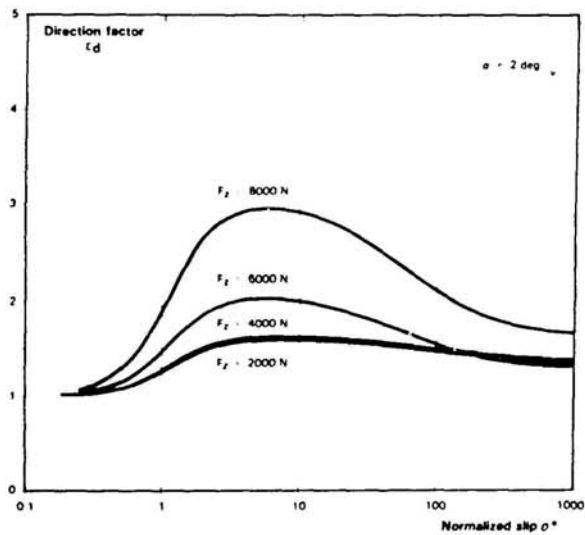


Fig. 17 - Direction factor as a function of  $\sigma^*$  as derived from measured data for a slip angle of 2 degrees.

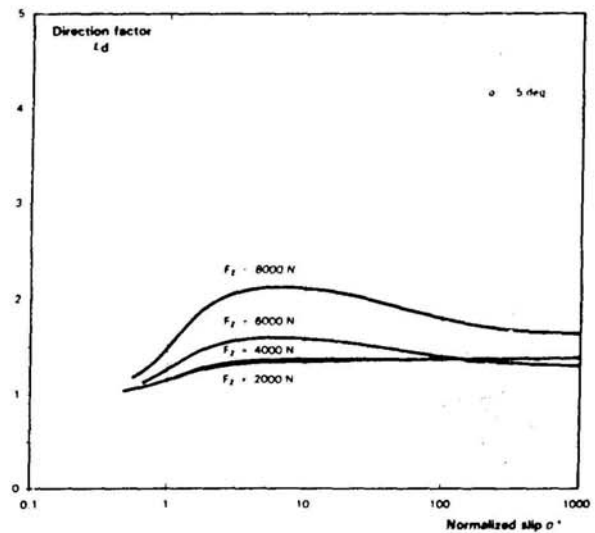


Fig. 18 - Direction factor as a function of  $\sigma^*$  as derived from measured data for a slip angle of 5 degrees.

$$\begin{aligned} \sigma_x^* &= \sigma_x / \sigma_{xm} \\ \sigma_y^* &= \sigma_y / \sigma_{ym} \\ \sigma^* &= \sqrt{\sigma_x^{*2} + \sigma_y^{*2}} \end{aligned} \quad (19)$$

The basic curves, but now as a function of  $\sigma^*$  have been shown in Fig. 15. On both characteristics ( $F_{x0}$  and  $F_{y0}$ ), partial slipping occurs for values of  $\sigma^*$  smaller than 1 and total sliding for values larger than 1. With  $\sigma^*$  as the new slip the equations (18) become:

$$\begin{aligned} F_x &= -(\sigma_x^* / \sigma^*) F_{x0}(\sigma^*) \\ F_y &= -(\sigma_y^* / \sigma^*) F_{y0}(\sigma^*) \\ F &= \sqrt{F_x^2 + F_y^2} \end{aligned} \quad (20)$$

The direction of the total force is now based on the direction of  $\sigma^*$ . For small values of  $\sigma^*$ , Eq. (20) is correct since then the forces will be independent and the linear relations hold:

$$\begin{aligned} F_{x0} &= C_{Fk} \sigma_{xm} \sigma^* \\ F_x &= -(\sigma_x^* / \sigma^*) F_{x0}(\sigma^*) \\ &= -(\sigma_x^* / \sigma^*) C_{Fk} \sigma_{xm} \sigma^* \\ &= -C_{Fk} \sigma_x \end{aligned} \quad (21)$$

and for  $F_y$  after a similar calculation:

$$F_y = -C_{Fa} \sigma_y \quad (22)$$

with  $C_{Fk}$  and  $C_{Fa}$  the longitudinal slip and the cornering stiffness respectively.

However, for large values of  $\sigma^*$  and equal friction coefficient ( $\mu$ ) in x and y direction, the total force should be in the opposite direction of the slip speed vector (and thus  $\bar{\sigma}$ ).

$$\begin{aligned} F_{x0} &= \mu F_z \\ F_x &= -(\sigma_x / \sigma) F_{x0}(\sigma^*) \\ &= -(\sigma_x / \sigma) \mu F_z \end{aligned} \quad (23)$$

and similarly for  $F_y$ :

$$F_y = -(\sigma_y / \sigma) \mu F_z \quad (24)$$

So with small slip,  $\sigma^*$  should be used to determine the direction of the total horizontal force and with large slip,  $\sigma$  should be used. Obviously, a need exists for an additional factor which controls the direction of the total horizontal force. This direc-

tion factor ( $\epsilon_d$ ), when introduced, yields:

$$F_x = -(\sigma_x^* / \sigma^*) F_{x0}(\sigma^*) \quad (25)$$

$$F_y = -\epsilon_d (\sigma_y^* / \sigma^*) F_{y0}(\sigma^*) \quad (26)$$

Figure 16 shows the construction of the total horizontal force. The magnitude of  $\epsilon_d$  will be 1 for small values of  $\sigma^*$  and  $\sigma_{ym} / \sigma_{xm}$  for large values of  $\sigma^*$ . For intermediate values of  $\sigma^*$  the value for  $\epsilon_d$  is determined from the measured relationships during combined cornering and braking. Figures 17 and 18 show examples of the variation of  $\epsilon_d$  ( $\sigma^*, F_z, \alpha$ ) for different loads and slip angles.

Because of the action of the brake force, the resulting cornering stiffness of the tyre appears to become larger. For this reason, the basic normalized side force characteristic has been given an initial slope which is a function of the brake force. This can easily be achieved by adjusting the coefficient B for the side force. The increment of B is:

$$\Delta B = -\beta F_x B \quad (\beta > 0) \quad (27)$$

with  $\beta$  denoting the longitudinal force sensitivity of the cornering stiffness.

Further study is required to explain the physical background of  $\beta$  and of the course of  $\epsilon_d$ , specially at high loads.

Figures 19 until 22 show comparisons between measurements and calculations for a tyre in various situations during combined cornering and braking. The graphs depict the variations of the brake force and the side force as a function of longitudinal slip and also the side force as a function of the brake force. To be able to compare calculations and measurements, the measured brake forces were corrected for the rolling resistance (vertical shift). With the aid of  $\epsilon_d$  and adjustment of B (side force), the model gives a good description of the measurements.

**SELF ALIGNING TORQUE DURING COMBINED CORNERING AND BRAKING** - To obtain the self aligning torque during combined cornering and braking, the side force has first to be multiplied by the pneumatic trail ( $t$ ). The pneumatic trail has been derived as a function of  $\alpha$  (or  $\tan \alpha$ ) during pure cornering. The deflection distribution over the contact length during combined cornering and braking is equal to the distribution during pure cornering if  $\tan \alpha = \sigma$  (cf.

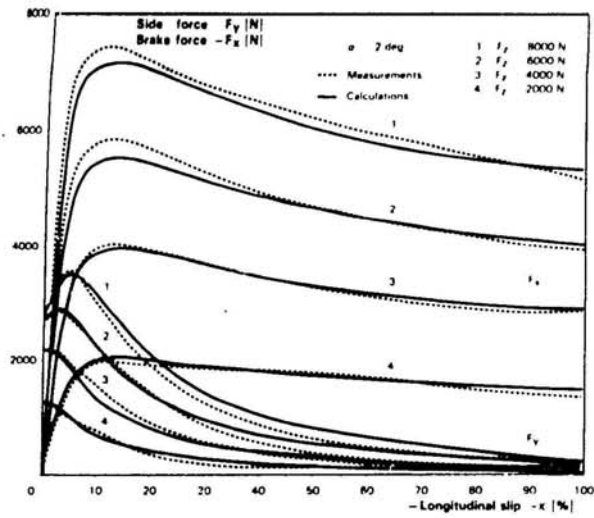


Fig. 19 - Side force and brake force vs longitudinal slip at 2 degrees slip angle.

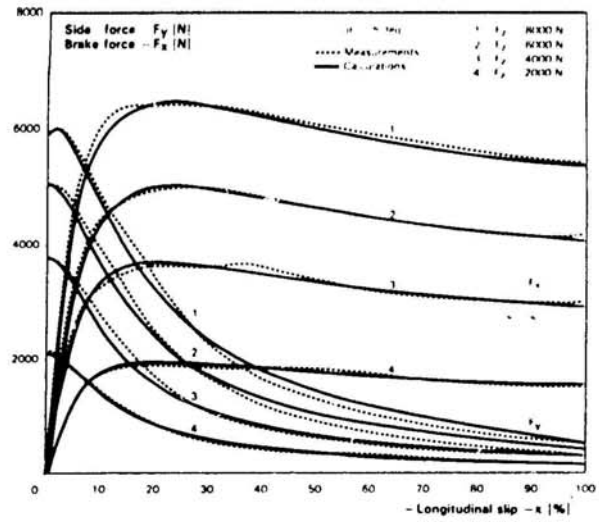


Fig. 20 - Side force and brake force vs longitudinal slip at 5 degrees slip angle.

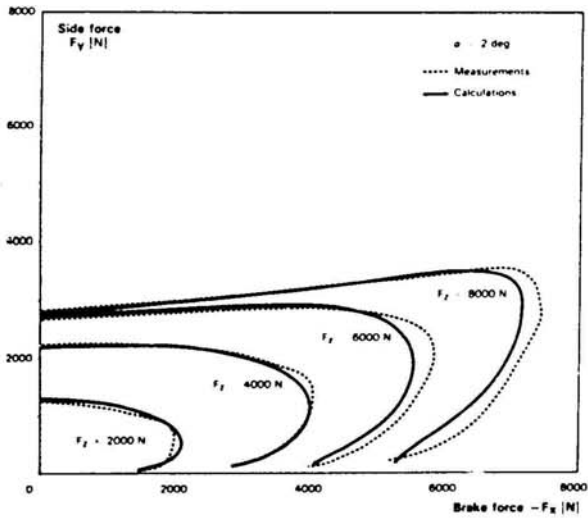


Fig. 21 - Side force vs brake force at 2 degrees slip angle.

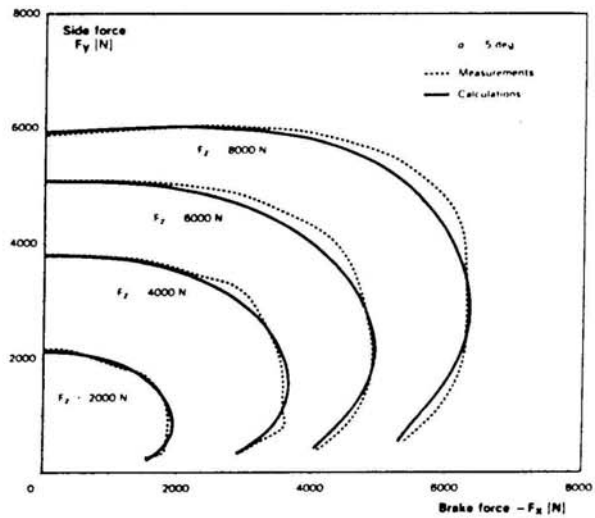


Fig. 22 - Side force vs brake force at 5 degrees slip angle.

[3]). Consequently instead of  $t$  ( $\tan \alpha$ ) we may write  $t(\sigma)$  which can be converted into  $t(\sigma^*)$ . The self aligning torque now becomes:

$$M_z' = -t(\sigma^*) F_y \quad (28)$$

Due to carcass compliance, the lines of action of both the side force and the brake force will be shifted which causes a contribution to the self aligning torque:

$$M_z = M_z' - s F_x F_y \quad (29)$$

with

$$s = \frac{1}{C_{cy}} - \frac{1}{C_{cx}} \quad (30)$$

$C_{cx}$  and  $C_{cy}$  denoting the longitudinal and lateral carcass stiffnesses respectively.

Figures 23 and 24 show comparisons between calculations and measurements. The measured characteristics have been corrected for an apparently constant offset of the line of action of the brake force of approx. 15 mm. This means that even with a slip angle of zero, a large self aligning torque is present. The overturning couple ( $M_x$ ) was not measured, so no information is available about the offset of the vertical force which may have caused this. The measured values shown in Figs. 23 and 24 have been corrected for this phenomenon, which is not yet fully understood.

**POSSIBLE EXTENSIONS** - The model so far developed, including interaction between side and brake force, may be extended with camber and positive longitudinal slip (driving), for instance, if measurements in these conditions are available. The measurements described earlier did not include these combinations of input.

## CONCLUSION AND SUMMARY

The proposed formula turns out to be not only very accurate in describing the measured data. It also characterizes some of the typifying quantities of the tyre such as slip stiffnesses and peak values and permits the calculation of forces and torque in conditions which deviate from those imposed during the actual measurements. Compared with the conventional way of representing tyre data by polynomials with coefficients which have no direct physical meaning, this way of representing tyre data seems to be a big step in the right direction.

The results of the model which describes the behaviour of the tyre during combined cornering

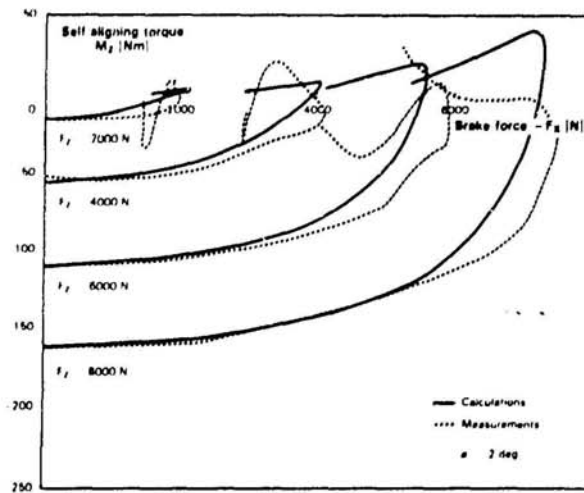


Fig. 23 - Self aligning torque vs brake force at 2 degrees slip angle.

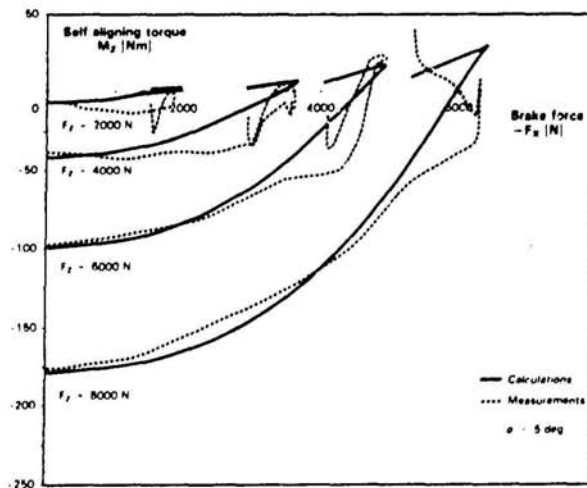


Fig. 24 - Self aligning torque vs brake force at 5 degrees slip angle.



and braking are very similar to the measurements which were carried out in these conditions. This means that the representation of the tyre data which is valid in pure conditions can also be used to provide information for a combined condition if a new slip quantity is used: the normalized slip.

Because of the physical meaningful coefficients of the representation, it is easy to vary some of the typifying quantities of the tyre. Simulations may then be carried out with a hypothetical tyre. In this way, the performance of a specific vehicle can be predicted.

The described mathematical representation is just the beginning of an effort to describe tyre behaviour in a way which is accurate, compact, physically meaningful and easy to use. By continuing this effort, hopefully, the tyre will be given a sufficiently complete representation in vehicle models as accurate as justified by the great importance the tyre has in controlling the horizontal motion and therefore in the Dynamic Safety of the vehicle.

## REFERENCES

1. A. Sitchin, "Acquisition of Transient Tire Force and Moment Data for Dynamic Vehicle Handling Simulations", SAE Paper No. 831790, November 7-10, 1983
2. G. Ruf, "Theoretische Untersuchungen des Federungsverhaltens von Vierrad-Strassenfahrzeugen", Fortschr.-Ber. VDI-Z Reihe 12 No. 44 104-105, Dusseldorf 1983
3. H.B. Pacejka, "Modelling of the Tyre as a Vehicle Component with Applications", Lehr-gang V 2.01, Carl-Cranz-Gesellschaft, 1982
4. P. Lugner, R. Lorenz, E. Schindler, "The Connection of Theoretical Simulation and Experiments in Passenger Car Dynamics", Proc. 8th IAVSD Symp. on the dynamics of vehicles, Cambridge, Mass., August 15-19, 1983, ed. J.K. Hedrick, Swets & Zeitlinger B.V., Lisse Neth., 1984

## APPENDIX

### PROPOSED TYRE FORMULAE

#### SIDE FORCE:

$$F_y = D \sin(C \arctan(B\phi)) + \Delta S_v$$

with

$$\phi = (1-E)(\alpha + \Delta S_h) + (E/B) \arctan(B(\alpha + \Delta S_h))$$

$$D = a_1 F_z^2 + a_2 F_z$$

$$C = 1.30$$

$$B = \left( \frac{a_3 \sin(a_4 \arctan(a_5 F_z))}{CD} \right) (1 - a_{12} |\gamma|)$$

$$E = a_6 F_z^2 + a_7 F_z + a_8$$

$$\Delta S_h = a_9 \gamma$$

$$\Delta S_v = (a_{10} F_z^2 + a_{11} F_z) \gamma$$

#### SELF ALIGNING TORQUE:

$$M_z = D \sin(C \arctan(B\phi)) + \Delta S_v$$

with

$$\phi = (1-E)(\alpha + \Delta S_h) + (E/B) \arctan(B(\alpha + \Delta S_h))$$

$$D = a_1 F_z^2 + a_2 F_z$$

$$C = 2.40$$

$$B = \left( \frac{a_3 F_z^2 + a_4 F_z}{C D e^{a_5 F_z}} \right) (1 - a_{12} |\gamma|)$$

$$E = (a_6 F_z^2 + a_7 F_z + a_8) / (1 - a_{13} |\gamma|)$$

$$\Delta S_h = a_9 \gamma$$

$$\Delta S_v = (a_{10} F_z^2 + a_{11} F_z) \gamma$$

#### BRAKE FORCE:

$$F_x = D \sin(C \arctan(B\phi))$$

with

$$\phi = (1-E) \kappa + (E/B) \arctan(B\kappa)$$

$$D = a_1 F_z^2 + a_2 F_z$$

$$C = 1.65$$

$$B = \frac{a_3 F_z^2 + a_4 F_z}{C D e^{a_5 F_z}}$$

$$E = a_6 F_z^2 + a_7 F_z + a_8$$

The values for the coefficients  $a_1$  until  $a_8$  are tabulated in Table 2 and for  $a_9$  until  $a_{13}$  in Table 3.